Electronic Supplementary Information (New Journal of Chemistry)

The thermal response of lead sensitized terbium emission in group II sulfide nanoparticles: importance of spatial proximity and band gap engineering

Madhumita Bhar,[1] Nayan Bhunia[1] and Prasun Mukherjee[1,*]

[1] Centre for Research in Nanoscience and Nanotechnology, University of Calcutta, JD-2, Sector-III, Salt Lake, Kolkata-700106, West Bengal, India

E-mail: pmcrnn@caluniv.ac.in, pmukherjee12@gmail.com

Materials and Methods

Chemicals. 3-mercapto-1,2-propanediol (1-TG) (90+%), thiourea (99%), terbium acetate hydrate (99.9%), cadmium acetate hydrate ($\geq$ 98.0%), and lead nitrate (99%) were purchased from Alfa Aesar. Coumarin 153 (C153), potassium iodide ($\geq$ 99.0%), zinc acetate dihydrate (98%), N,N-dimethyl formamide (DMF) were purchased from Merck. Methanol was purchased from Finar. All these chemicals were used without further purification. Argon used during the synthesis was purchased from Hindustan Gases and Weldings. Millipore water used in the synthesis and sample preparation was obtained from a system maintaining resistivity of 18.2 MΩ cm at 25°C.

Synthesis of Nanoparticles. Hydrophilic Zn(Tb)S and Cd(Tb)S NPs were synthesized following a synthetic procedure proposed by Sarma and coworkers, [1] and Weller and coworkers, [2] respectively, with further modification accompanied by the incorporation of lanthanides in these NPs. [3-6] Typically, to perform the synthesis of the Zn(Tb)S NPs with 10% terbium cation as dopant, 1.98 mmol of zinc acetate dihydrate, 0.22 mmol of terbium acetate hydrate, 1.56 mmol of thiourea, and 50 ml of DMF as solvent were taken in a 100 ml three neck round bottom flask. The whole mixture was maintained at room temperature with stirring under argon atmosphere. 2.72 mmol of 1-thioglycerol (1-TG) was added to the mixture at a raised temperature. This mixture was refluxed for eight hours at 140°C under argon atmosphere. The mixture was then collected and cooled to room temperature. These synthesized NPs were collected by precipitation with the addition of acetone. The purification process was performed two times at 4000 rpm for 20 minutes to remove unreacted reagents. Similar procedure was utilized to synthesize the Cd(Tb)S NPs, where cadmium acetate hydrate was used as cadmium source instead of the zinc precursor.

Postsynthetic Modification. Zn(Tb)S NPs were modified postsynthetically by adding lead nitrate solution to an aqueous dispersion of the Zn(Tb)S NPs of known concentration in a

volume by volume ratio. This sample is labeled as Zn(Tb)S/Pb. To be particular, to prepare Zn(Tb)S/Pb NPs with a relative reactant concentration ratio of [Zn(Tb)S] : [Pb^{2+}] = $1:10^{-2}$, a known concentration of 0.04 mM Zn(Tb)S (measured using molar extinction coefficient of the NPs as 1.2×10^3 $M^{-1}cm^{-1}$ at 270 nm [7]) was mixed with 0.04×10^{-2} mM of lead nitrate solution in equal volume. The postsynthetically modified aqueous dispersion was kept at room temperature for approximately 24 hours. It was further purified with acetone under centrifugation at 4000 rpm for 20 minutes to ensure the complete removal of any unreacted precursors. This purified material was dispersed in water to acquire photoluminescence spectra. The Cd(Tb)S NPs were also modified postsynthetically following the same procedure.

2×10^{-6} (M) stock solution of coumarin (C153) in methanol was prepared by diluting a stock solution. 0.4 (M) potassium iodide was added to the C153 solution for quenching. This solution was used for further photoluminescence experiments.

Transmission Electron Microscopy. Transmission electron microscopy (TEM) measurements of the materials investigated were performed by using a TEM instrument (Make: JEOL, Model: JEM-2100). The instrument was operated with an acceleration potential of 200 kV. A small quantity of aqueous dispersion of the sample was placed on a carbon coated copper grid for TEM measurements. The grid was dried before measurements.

Energy Dispersive X-Ray Spectroscopy. Zeiss EVO 18 eV scanning electron microscopy instrument was used to collect the energy dispersive X-ray spectra (EDS) of the NPs. All EDS measurements were performed with the purified NPs.

X-Ray Photoelectron Spectroscopy. X–ray photoelectron spectra (XPS) were collected using ULVAC PHI Inc., VERSA PROBE (iv), USA. All XPS measurements were performed with the purified NPs.

X-Ray Diffraction. PANanalytical X'pert PRO diffractometer was used to study X-ray diffraction (XRD) pattern. A generator voltage of 45 kV and a current of 40 mA with Cu Kα radiation (λ = 0.154 nm) was used to operate this diffractometer. Temperature induced structural alterations (if any) was evaluated by performing experiments with samples prepared at 293 K and with the samples that were pretreated at 333 K. For this, the purified Zn(Tb)S and Zn(Tb)S/Pb NPs dispersions were heated at 333 K, cooled to room temperature and purified with acetone to remove free ions. The diffraction patterns were acquired from 20° to 80° range for all the NPs.

Fourier Transform Infrared (FTIR) Spectroscopy. Fourier transform infrared (FTIR) spectra of the samples were acquired using a Jasco FTIR 6300 spectrometer. Each spectrum was acquired with an average of 64 scans. The resolution was maintained at 4 cm^{-1}. The samples were prepared by a standard KBr pellet method. All the measurements were performed at room temperature.

Electronic Spectroscopy.   The absorption spectra in the ultraviolet-visible range were acquired with the PerkinElmer Lambda 1050 absorption spectrophotometer in the spectral range 250 to 800 nm. The spectra were collected using a 2 nm band pass.

A Horiba Fluorolog 3-22 photoluminescence spectrometer was used to collect the photoluminescence spectra at room temperature. The photoluminescence spectra at various temperatures were acquired by connecting the spectrometer to a temperature controller (Make: Newport, Model: 350B). The Zn(Tb)S and Zn(Tb)S/Pb NPs were excited at 280 nm to acquire the photoluminescence emission spectra. The excitation spectra were collected monitoring the broad NP emission around 400 nm and the sharp terbium related band at 545 nm. Both the emission and excitation slit width were maintained at 4 nm. To acquire the time-gated emission spectra for Cd(Tb)S and Cd(Tb)S/Pb, the NPs were excited at 280 nm keeping both the slit widths at 14 nm. Coumarin 153 (C153) solutions were excited at 420

nm to collect the emission spectra. The corresponding excitation spectra were acquired monitoring the emission at 600 nm. In these acquisitions, slit widths of 2 nm for both the excitation and emission monochromators were used. In all the measurements, the emission spectra were corrected for lamp and detector response. The excitation spectra were corrected for lamp response. Absorption corrected integrated emission intensity were used to obtain the emission quantum yield of Tb^{3+} by a relative method, using a reference value of emission quantum yield for coumarin 153 (C153) dissolved in methanol taken as 0.42. [8, 9] The sole emission contribution of Tb^{3+} was extracted from the steady-state emission spectra. For example, from the emission spectra of the Zn(Tb)S NPs, to extract the Tb^{3+} emission band at 545 nm, the spectrum was first interpolated with two data points in the wavelength range of 520 – 570 nm. This was next interpolated with a 1 nm data interval, the same as was used for experimental spectral acquisition. This interpolated line was then subtracted from the experimentally acquired spectrum to obtain the terbium emission contribution.

The time-gated and time-resolved spectra were collected using the same instrument using a pulsed xenon lamp, with a delay and gate time of 0.05 ms and 5 ms, respectively. All the NPs were excited at 280 nm. The 0.05 ms delay time ensures complete decay of NPs emission. [8] All the electronic spectroscopy experiments were performed using the purified NPs.
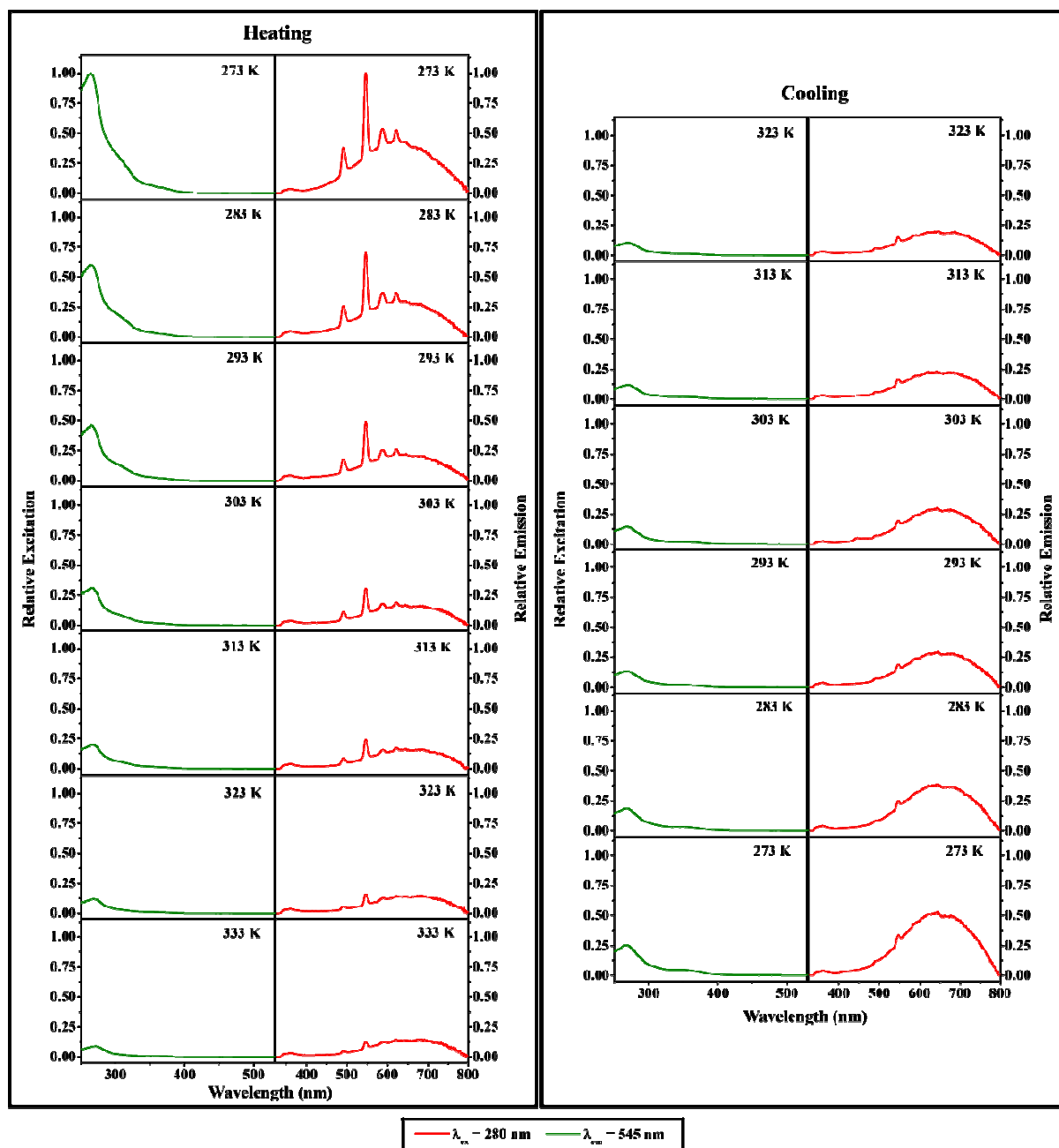
Figure S1. Representative excitation and emission spectra in the Zn(Tb)S/Pb NPs as a function of temperature. The emission around 650 nm can be correlated with a $^3P_0 \rightarrow {}^1S_0$ transition at the Pb^{2+} center.
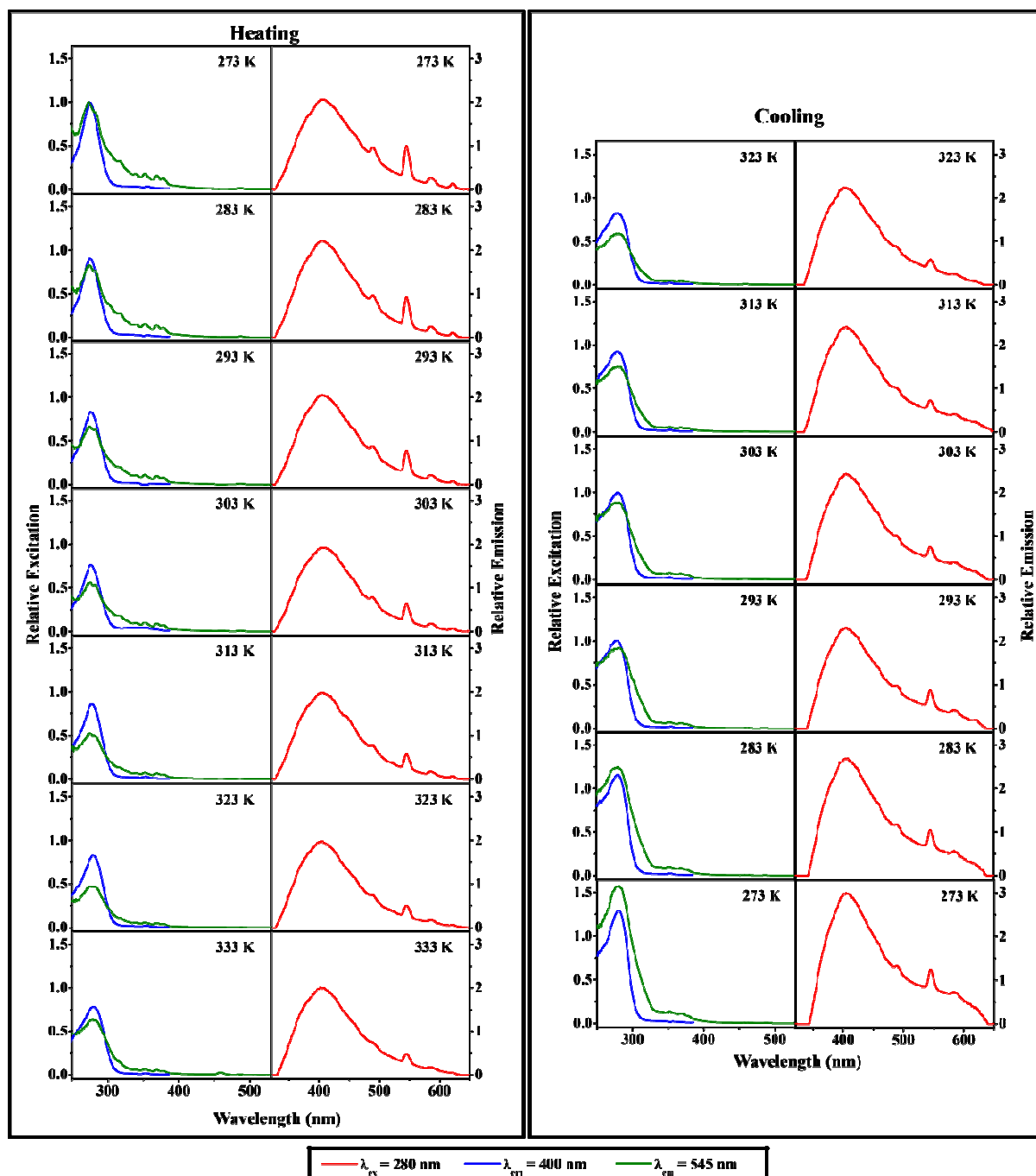
Figure S2. Representative excitation and emission spectra in the Zn(Tb)S NPs as a function of temperature.
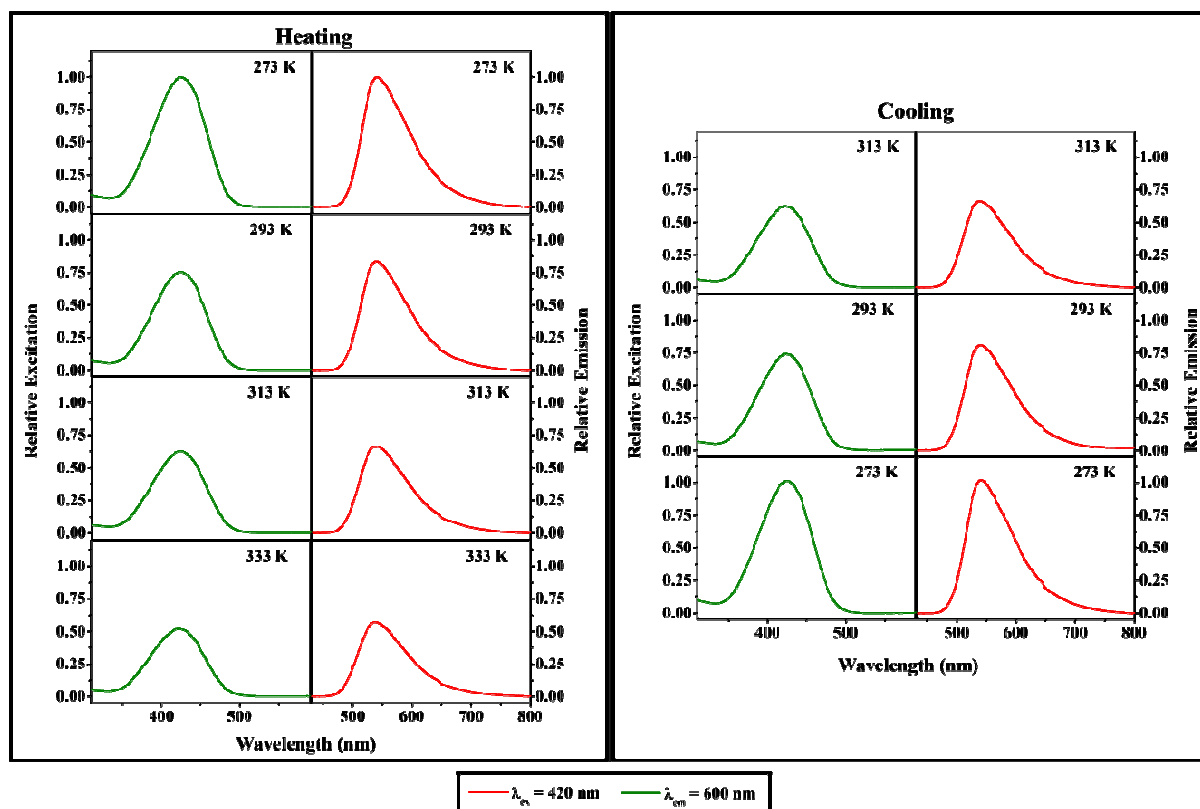
Figure S3. Representative excitation and emission spectra of C153 in methanol with Γ as an emission quencher.
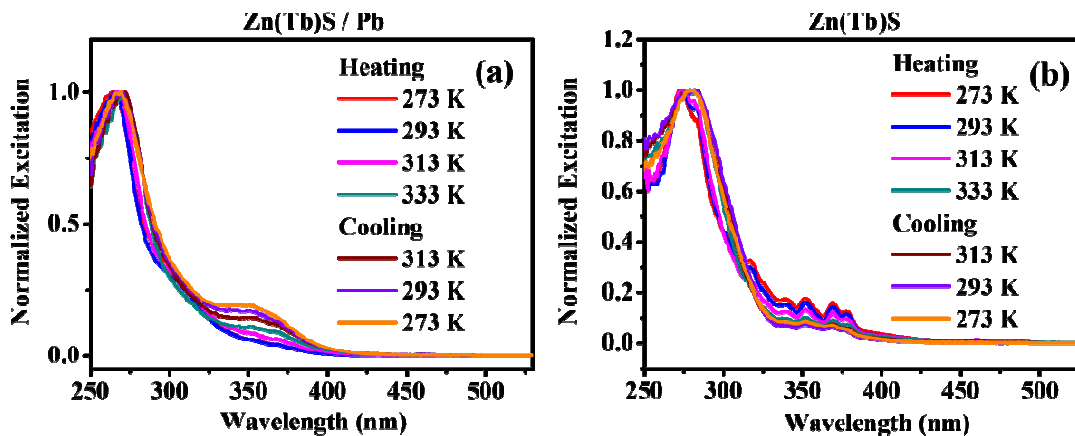
Figure S4. A comparison of normalized excitation spectra of the Zn(Tb)S/Pb and Zn(Tb)S NPs as a function of temperature is shown.
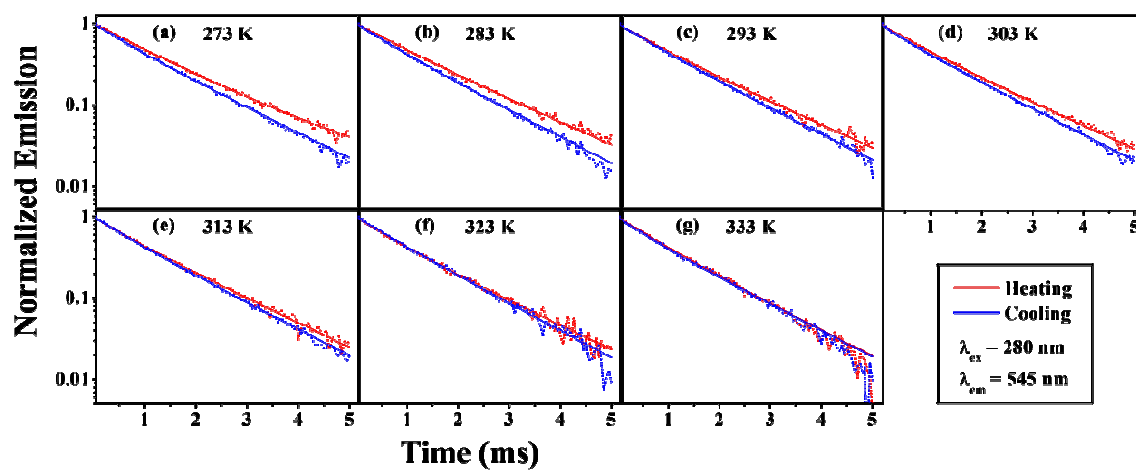
Figure S5. Tb^{3+} emission lifetime decay profiles in the Zn(Tb)S/Pb NPs are shown.
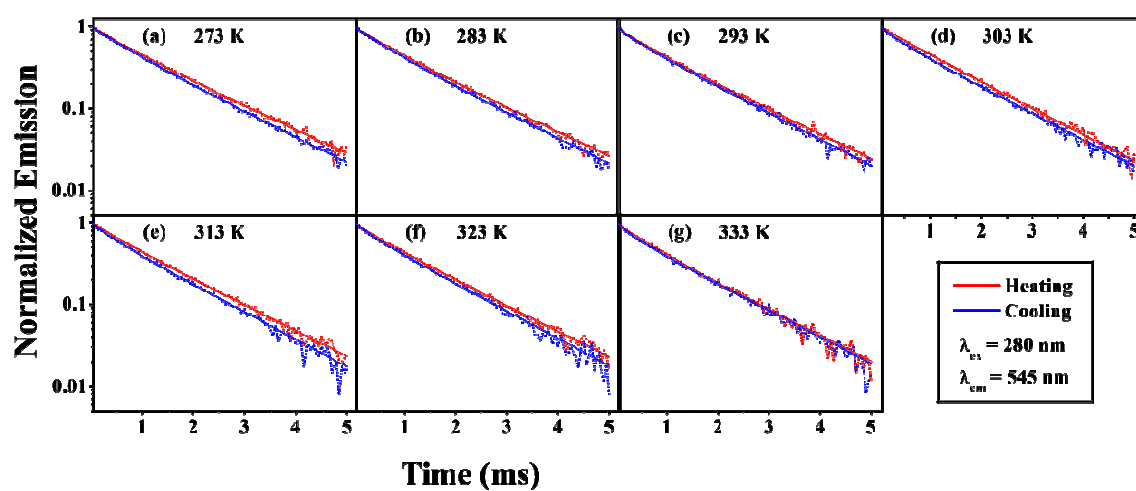
Figure S6. Tb^{3+} emission lifetime decay profiles in the Zn(Tb)S NPs are shown.

Table S1. Tb^{3+} Emission Lifetime Fitting Parameters.[a]

Temperature (K)	a_S	τ_S (ms)	a_L	τ_L (ms)	$<\tau>$ (ms)
Zn(Tb)S					
273	0.24 ± 0.02	0.74 ± 0.03	0.76 ± 0.02	1.51 ± 0.01	1.33 ± 0.04
283	0.29 ± 0.02	0.74 ± 0.02	0.71 ± 0.02	1.51 ± 0.01	1.29 ± 0.04
293	0.25 ± 0.01	0.62 ± 0.02	0.75 ± 0.01	1.46 ± 0.01	1.25 ± 0.02
303	0.24 ± 0.02	0.96 ± 0.01	0.76 ± 0.02	1.41 ± 0.01	1.30 ± 0.04
313	0.22 ± 0.03	0.70 ± 0.04	0.78 ± 0.03	1.44 ± 0.02	1.28 ± 0.05
323	0.24 ± 0.03	0.66 ± 0.04	0.76 ± 0.03	1.44 ± 0.02	1.25 ± 0.05
333	0.24 ± 0.02	0.59 ± 0.03	0.76 ± 0.02	1.37 ± 0.01	1.18 ± 0.03
Reverse 333	0.27 ± 0.01	0.45 ± 0.01	0.73 ± 0.01	1.39 ± 0.01	1.14 ± 0.02
Reverse 323	0.16 ± 0.02	0.37 ± 0.04	0.84 ± 0.02	1.29 ± 0.02	1.14 ± 0.03
Reverse 313	0.17 ± 0.03	0.37 ± 0.04	0.83 ± 0.03	1.29 ± 0.02	1.13 ± 0.04
Reverse 303	0.19 ± 0.02	0.43 ± 0.04	0.81 ± 0.02	1.34 ± 0.02	1.17 ± 0.03
Reverse 293	0.17 ± 0.02	0.43 ± 0.03	0.83 ± 0.02	1.33 ± 0.04	1.18 ± 0.04
Reverse 283	0.28 ± 0.02	0.66 ± 0.02	0.72 ± 0.03	1.41 ± 0.02	1.20 ± 0.03
Reverse 273	0.29 ± 0.02	0.70 ± 0.01	0.71 ± 0.02	1.44 ± 0.01	1.23 ± 0.03
Zn(Tb)S/Pb					
273	0.22 ± 0.01	0.80 ± 0.02	0.78 ± 0.01	1.61 ± 0.01	1.43 ± 0.02
283	0.22 ± 0.02	0.82 ± 0.02	0.78 ± 0.02	1.56 ± 0.01	1.40 ± 0.04
293	0.27 ± 0.01	0.72 ± 0.01	0.73 ± 0.01	1.56 ± 0.01	1.33 ± 0.02
303	0.23 ± 0.01	0.71 ± 0.02	0.77 ± 0.01	1.51 ± 0.01	1.33 ± 0.02
313	0.24 ± 0.02	0.60 ± 0.04	0.76 ± 0.02	1.46 ± 0.02	1.25 ± 0.04
323	0.22 ± 0.01	0.54 ± 0.02	0.78 ± 0.01	1.41 ± 0.01	1.22 ± 0.02
333	0.25 ± 0.03	0.71 ± 0.03	0.75 ± 0.03	1.36 ± 0.01	1.20 ± 0.04
Reverse 333	0.21 ± 0.02	0.53 ± 0.03	0.79 ± 0.02	1.34 ± 0.01	1.17 ± 0.03
Reverse 323	0.22 ± 0.03	0.73 ± 0.03	0.78 ± 0.03	1.34 ± 0.01	1.21 ± 0.04
Reverse 313	0.21 ± 0.02	0.64 ± 0.03	0.79 ± 0.02	1.36 ± 0.01	1.21 ± 0.03
Reverse 303	0.22 ± 0.01	0.54 ± 0.02	0.78 ± 0.01	1.39 ± 0.01	1.20 ± 0.01
Reverse 293	0.24 ± 0.02	0.75 ± 0.03	0.76 ± 0.02	1.39 ± 0.01	1.24 ± 0.04
Reverse 283	0.25 ± 0.02	0.70 ± 0.02	0.75 ± 0.02	1.37 ± 0.01	1.20 ± 0.03
Reverse 273	0.24 ± 0.02	0.64 ± 0.02	0.76 ± 0.02	1.41 ± 0.01	1.23 ± 0.03

[a] The lifetime fitting parameters are reported as average and standard deviation from two measurements with independent post-synthetic modifications of the NPs.
[b] $<\tau> = a_s\tau_S + a_L\tau_L$. $R^2 \geq 0.997$.

Table S2. The Elemental Composition of the Zn(Tb)S Based NPs.[a]

Sample temperature	Elements			
	Zn	**Tb**	**S**	**Pb**
Zn(Tb)S				
273 K	26.4 ± 1.7	6.0 ± 0.3	67.6 ± 1.5	----
293 K	33.8 ± 0.8	5.6 ± 0.5	60.6 ± 0.6	----
313 K	45.0 ± 2.3	3.9 ± 0.1	51.1 ± 2.2	----
333 K	44.4 ± 1.6	4.1 ± 0.1	51.5 ± 1.7	----
Zn(Tb)S/Pb				
273 K	27.9 ± 1.8	7.7 ± 0.7	59.0 ± 1.3	5.4 ± 0.5
293 K	31.6 ± 0.8	7.3 ± 0.3	56.2 ± 1.4	4.9 ± 0.5
313 K	46.5 ± 1.8	3.0 ± 0.3	46.2 ± 1.8	4.3 ± 0.4
333 K	45.6 ± 0.1	2.6 ± 0.1	47.4 ± 0.1	4.4 ± 0.2

[a] Values are reported as average and standard deviation from elemental compositions obtained from three different spatial locations.
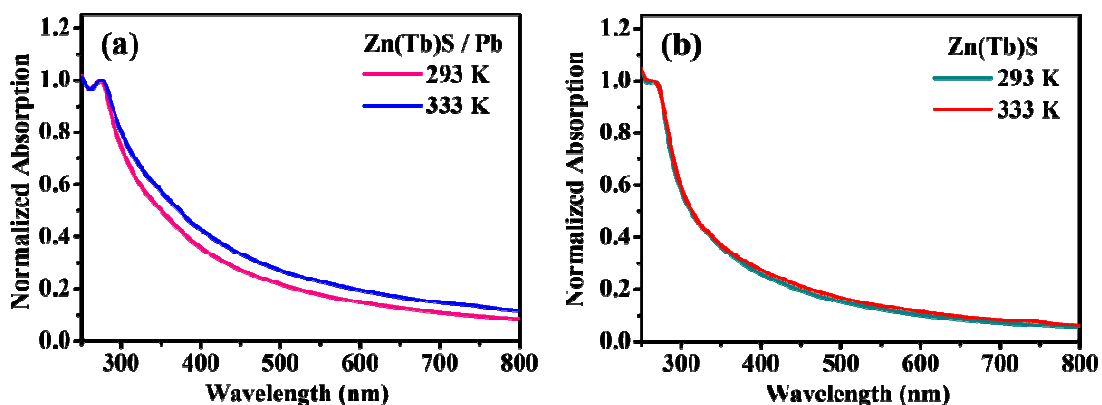
Figure S7. The electronic absorption spectra of the Zn(Tb)S/Pb and Zn(Tb)S NPs are shown. The NPs are either treated at 293 K, or are pre-treated at 333 K following the spectral acquisition at 293 K.
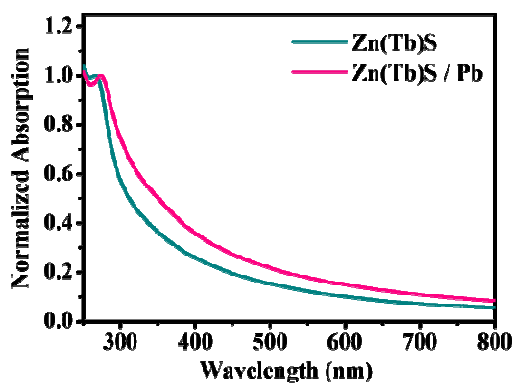
Figure S8. A comparison between the electronic absorption spectra of the Zn(Tb)S and Zn(Tb)S/Pb NPs is shown.
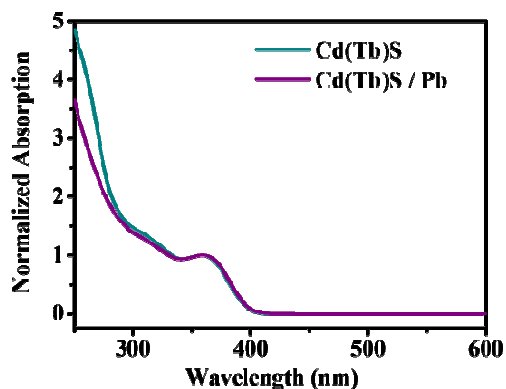
Figure S9. Electronic absorption spectra of the 1-TG capped Cd(Tb)S and Cd(Tb)S/Pb NPs are shown.
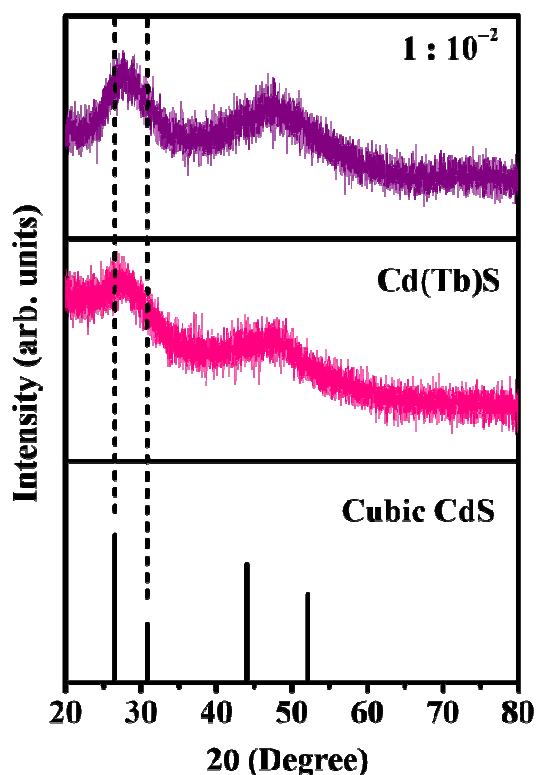
Figure S10. XRD profiles for the Cd(Tb)S NPs and the Cd(Tb)S/Pb NPs with [Cd(Tb)S] : $[Pb^{2+}] = 1:10^{-2}$.

Table S3. The Elemental Composition of the Cd(Tb)S Based NPs.[a]

Sample	Elements			
Cd(Tb)S				
Cd(Tb)S (293 K)	35.2 ± 0.5	4.7 ± 0.3	60.1 ± 0.3	--
Cd(Tb)S (333 K)	35.6 ± 0.1	4.9 ± 0.2	59.5 ± 0.3	--
Cd(Tb)S/Pb				
Cd(Tb)S/Pb (293 K)	37.4 ± 0.1	4.0 ± 0.1	56.2 ± 0.1	2.4 ± 0.1
Cd(Tb)S/Pb (333 K)	37.6 ± 0.4	4.4 ± 0.7	55.6 ± 1.0	2.4 ± 0.2

[a] Values are reported as average and standard deviation from elemental compositions obtained from three different spatial locations.

References

1.   J. Nanda, S. Sapra, D. D. Sarma, N. Chandrasekharan and G. Hodes, *Chem. Mater.*, 2000, **12**, 1018-1024.
2.   T. Vossmeyer, L. Katsikas, M. Gienig, I. G. Popovic, K. Diesner, A. Chemseddine, A. Eychmüller and H. Weller, *J. Phys. Chem.*, 1994, **98**, 7665-7673.
3.   A. Chakraborty, G. H. Debnath, M. Ahir, S. Bhattacharya, P. Upadhyay, A. Adhikary and P. Mukherjee, *RSC Adv.*, 2016, **6**, 43304-43315.
4.   S. Rudra, G. H. Debnath and P. Mukherjee, *RSC Adv.*, 2018, **8**, 18093-18108.

5.   S. Rudra, M. Bhar and P. Mukherjee, *J. Phys. Chem. C*, 2019, **123**, 29445-29460.
6.   M. Bhar, S. Rudra and P. Mukherjee, *J. Phys. Chem. C*, 2020, **124**, 6588-6597.
7.   P. Calandra, M. Goffredi and V. T. Liveri, *Colloids and Surfaces A: Physicochemical and Engineering Aspects*, 1999, **160**, 9-13.
8.   P. Mukherjee, C. M. Shade, A. M. Yingling, D. N. Lamont, D. H. Waldeck and S. Petoud, *J. Phys. Chem. A*, 2011, **115**, 4031-4041.
9.   J. E. Lewis and M. Maroncelli, *Chem. Phys. Lett.*, 1998, **282**, 197-203.